




REPORT

De novo variants in *PAK1* lead to intellectual disability with macrocephaly and seizures

 Susanne Horn,¹ Margaret Au,² Lina Basel-Salmon,^{3,4,5,6} Pinar Bayrak-Toydemir,⁷ Alexander Chapin,⁸ Lior Cohen,^{3,4,5,6} Mariet W. Elting,⁹ John M. Graham, Jr,² Claudia Gonzaga-Jauregui,¹⁰ Osnat Konen,^{5,11} Max Holzer,¹²  Johannes Lemke,¹ Christine E. Miller,⁸ Linda K. Rey,¹³  Nicole I. Wolf,¹⁴ Marjan M. Weiss,⁹ Quinten Waisfisz,⁹ Ghayda M. Mirzaa,^{15,16} Dagmar Wiczorek,¹³ Heinrich Sticht¹⁷ and Rami Abou Jamra¹

Using trio exome sequencing, we identified *de novo* heterozygous missense variants in *PAK1* in four unrelated individuals with intellectual disability, macrocephaly and seizures. *PAK1* encodes the p21-activated kinase, a major driver of neuronal development in humans and other organisms. In normal neurons, *PAK1* dimers reside in a trans-inhibited conformation, where each autoinhibitory domain covers the kinase domain of the other monomer. Upon GTPase binding via CDC42 or RAC1, the *PAK1* dimers dissociate and become activated. All identified variants are located within or close to the autoinhibitory switch domain that is necessary for trans-inhibition of resting *PAK1* dimers. Protein modelling supports a model of reduced ability of regular autoinhibition, suggesting a gain of function mechanism for the identified missense variants. Alleviated dissociation into monomers, autophosphorylation and activation of *PAK1* influences the actin dynamics of neurite outgrowth. Based on our clinical and genetic data, as well as the role of *PAK1* in brain development, we suggest that gain of function pathogenic *de novo* missense variants in *PAK1* lead to moderate-to-severe intellectual disability, macrocephaly caused by the presence of megalencephaly and ventriculomegaly, (febrile) seizures and autism-like behaviour.

- 1 Institute of Human Genetics, University Medical Center Leipzig, 04103 Leipzig, Germany
- 2 Department of Pediatrics, Cedars Sinai Medical Center, David Geffen School of Medicine at UCLA, Los Angeles, California, USA
- 3 Raphael Recanati Genetic Institute, Rabin Medical Center-Beilinson Hospital, Petach Tikva, Israel
- 4 Pediatric Genetics Clinic, Schneider Children's Medical Center of Israel, Petach Tikva 4920235, Israel
- 5 Sackler Faculty of Medicine, Tel Aviv University, Tel Aviv 6997801, Israel
- 6 Felsenstein Medical Research Center, Rabin Medical Center, Petach Tikva 4941492, Israel
- 7 Department of Pathology, University of Utah School of Medicine, Salt Lake City, UT, USA; ARUP Laboratories, Salt Lake City, UT, USA
- 8 ARUP Laboratories, Salt Lake City, UT, USA
- 9 Amsterdam UMC, Vrije Universiteit Amsterdam, Department of Clinical Genetics, De Boelelaan 1117, Amsterdam, The Netherlands
- 10 Regeneron Genetics Center, Regeneron Pharmaceuticals Inc., Tarrytown, NY, USA
- 11 Department of Pediatric Radiology, Schneider Children's Medical Center of Israel, Petach Tikva 4920235, Israel
- 12 Department for Molecular and Cellular Mechanisms of Neurodegeneration, Paul Flechsigs Institute for Brain Research, University of Leipzig, Leipzig, Germany
- 13 Institute of Human Genetics, University Hospital Duesseldorf, Heinrich-Heine-University Duesseldorf, Duesseldorf, Germany
- 14 Department of Child Neurology, Emma Children's Hospital, Amsterdam UMC, Vrije Universiteit Amsterdam, and Amsterdam Neuroscience, Amsterdam, The Netherlands
- 15 Center for Integrative Brain Research, Seattle Children's Research Institute, Seattle, Washington, USA
- 16 Department of Pediatrics, University of Washington, Seattle, Washington, USA
- 17 Institute of Biochemistry, Friedrich-Alexander-Universität Erlangen-Nürnberg, 91054 Erlangen, Germany

Received October 2, 2018. Revised June 7, 2019. Accepted July 4, 2019. Advance Access publication August 29, 2019

© The Author(s) (2019). Published by Oxford University Press on behalf of the Guarantors of Brain.

This is an Open Access article distributed under the terms of the Creative Commons Attribution Non-Commercial License (<http://creativecommons.org/licenses/by-nc/4.0/>), which permits non-commercial re-use, distribution, and reproduction in any medium, provided the original work is properly cited. For commercial re-use, please contact journals.permissions@oup.com

Correspondence to: Dr Susanne Horn
 Institute of Human Genetics, University Medical Center Leipzig, 04103 Leipzig, Germany
 E-mail: Susanne.Horn@medizin.uni-leipzig.de

Correspondence may also be addressed to: Dr Rami Abou Jamra
 E-mail: rami.aboujamra@medizin.uni-leipzig.de

Keywords: *de novo*; exome sequencing; intellectual disability; macrocephaly; seizures

Abbreviation: FXS = fragile X syndrome

Introduction

With a prevalence of about 1–3%, intellectual disability is a major health and socioeconomic issue (Maulik *et al.*, 2011). Intellectual disability is genetically highly heterogeneous, with each recognized cause affecting only a small fraction of all patients (Vissers *et al.*, 2016). Services for people with intellectual disability increasingly focus on innovative and personalized therapies. Major research efforts have used efficient molecular diagnostic tools for rare diseases, especially exome sequencing given its high diagnostic yield (Ligt *et al.*, 2012; Boycott *et al.*, 2017; Trujillano *et al.*, 2017), thus providing knowledge of specific genetic variants as a prerequisite for personalized therapy in cases where mechanistic insights on the affected genes and proteins exist.

At four centres in Germany, the Netherlands, the USA and Israel, we ascertained four unrelated individuals with a neurodevelopmental disorder, including intellectual disability, seizures and macrocephaly. We performed exome sequencing to identify the underlying genetic cause of the disease. Here we present data that indicate a pathogenic mechanism of *PAK1* mutations by a dominant gain-of-function effect. *De novo* *PAK1* missense pathogenic variants have also recently been described in two cases with intellectual disability, macrocephaly, seizures and speech delay (MIM: 618158) (Harms *et al.*, 2018). Human *PAK1* is a 545-amino acid (aa) protein with two major domains, an autoregulatory domain and a protein kinase domain (Fig. 1). In its inactive form, it homodimerizes by interacting and binding at a region within the autoregulatory domain (74–132 aa) masking the active site of the kinase. Therefore the autoregulatory domain is important for the autoinhibition of this kinase, and this mechanism has been well described for *PAK1* (Lei *et al.*, 2000; Parrini *et al.*, 2002; Pirruccello *et al.*, 2006). In the inhibited state, the inhibitory-switch domain of one homodimer overlaps the GTPase binding region (75–105 aa) of the other homodimer and a polypeptide segment covers the kinase cleft (Parrini *et al.*, 2002). During activation, GTPase binding triggers refolding of the inhibitory-switch domain, disrupting the *PAK1* dimer and leading to rearrangement of the kinase active site into a catalytically competent state.

We propose that *PAK1* disease-causing variants result in activation of the *PAK1*-LIMK1 pathway, a mechanism that

is discussed in fragile X syndrome (FXS) (Hayashi *et al.*, 2007; Pyronneau *et al.*, 2017).

Materials and methods

Subjects

Informed consent of all examined individuals and/or their guardians was obtained according to Institutional Review Board approved research protocols, including consent for publishing of the clinical as well as the genetic and genomic results. In Proband 4, genetic testing was carried out as part of routine clinical care and therefore institutional ethics approval was not required. Informed consent has been obtained for the published photo.

Exome sequencing

The study design comprised whole exome-sequencing (WES), genotype calling and the comparison of parent-offspring trios for the identification of rare variants in coding sequence associated with the observed human phenotype. We performed trio or family exome sequencing for all four probands and their biological parents according to standard methods (Supplementary material). Reported variants for all individuals were confirmed with Sanger dideoxynucleotide sequencing.

Protein modelling and analysis of gene expression

Energetic calculations of the observed protein changes were carried out using BindProfX (Xiong *et al.*, 2017) and visualized using UCSC Chimera v.1.12 (Pettersen *et al.*, 2004). To determine an unbiased set of relevant *PAK1* interacting genes for comparisons, we analysed gene expression in normal brain development using the R2 Genomics analysis and visualization platform (dataset brspv10rs). Interacting genes were predicted by using GENEMANIA (<https://genemania.org>).

Limitations of the study

Limitations of the retrospective case series are to be noted as there is limited information on the seizure types of the patients, with respect to detailed descriptions of seizures and post-ictal symptoms to classify them in more detail.

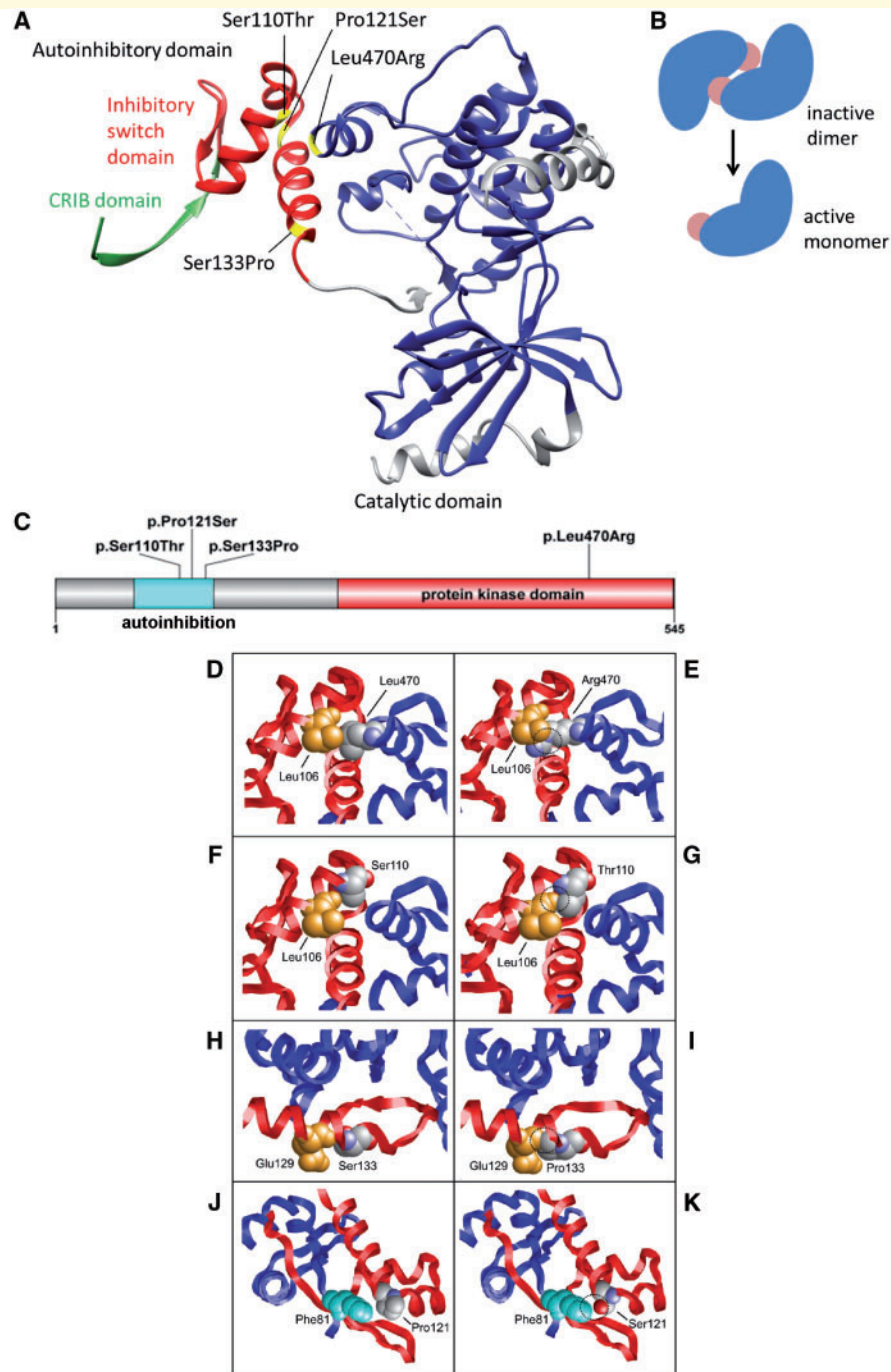


Figure 1 Structural effects of the PAK1 variants. (A) Protein structure of PAK1 with the catalytic domain (270–521 aa, blue) and the autoinhibitory domain (70–140 aa), comprising the Cdc42 Rac Interactive Binding (CRIB) domain (75–86 aa, green, <https://www.uniprot.org>) and the inhibitory switch domain (87–136 aa, red, <https://www.uniprot.org>). Variants Leu470Arg, Ser133Pro and Ser110Thr affect the contact zone of the catalytic and inhibitory switch domains. Pro121Ser is located in the interface between both PAK1 monomers (see also Supplementary Fig. 1). The CRIB domain (green) mediates activation of PAK1 by binding of RAC1 and CDC42. (B) Autoinhibition of PAK1. Autoinhibitory domains (light red) of inactive dimers cover the active site *in-trans*. After CDC42 or RAC1 binding, monomers dissociate, PAK1 autophosphorylation creates the active form of the protein. (C) Distribution of PAK1 variants across the coding region. (D and E) Leu470 forms tight hydrophobic interactions with Leu106, whereas the longer and charged Arg470 sidechain results in clashes with Leu106. In all panels the site of mutation is shown in space-filled presentation and coloured according to the atom types. Key interacting residues are shown in space-fill and are coloured orange or cyan. The two subunits of PAK1 are shown as red and blue ribbon, respectively. Sites of unfavourable interactions in the variants are highlighted by dashed circles. (F and G) Ser110 interacts with Leu106, whereas the additional methyl group present in the Thr110 sidechain forms clashes with Leu106. (H and I) Ser133 forms a backbone hydrogen bond with Glu129 within an α -helix. The presence of a cyclic sidechain in Pro133 results in a loss of this hydrogen bond and additionally causes steric clashes with Glu129. (J and K) Pro121 is located at a kink between two α -helices and near Phe81 of the second subunit. Replacement by a more flexible serine is expected to destabilize the kink and additionally creates an unfavourable interaction by placing the polar sidechain hydroxyl group in close proximity to the hydrophobic Phe81 sidechain.

Data availability

The authors confirm that the data supporting the findings of this study are available within the article and/or its Supplementary material.

Results

The probands presented with moderate to profound intellectual disability, seizures, macrocephaly, ventriculomegaly and other abnormalities in brain MRI, muscular hypotonia, and abnormal gait (Table 1, see detailed clinical descriptions in the Supplementary material). The analyses revealed *de novo* missense variants in *PAK1* in the four probands, c.1409T>G in exon 13 of 16 leading to p.(Leu470Arg) in Proband 1, and three changes in exon 4: c.397T>C; p.(Ser133Pro) in Proband 2, c.361C>T; p.(Pro121Ser) in Proband 3, and c.328T>A; p.(Ser110Thr) in Proband 4 (Table 1 and Supplementary Table 1). None of the variants in *PAK1* have been observed in the gnomAD database (accessed in September 2018) or in internal databases. All of the variants are predicted to be pathogenic by *in silico* bioinformatics prediction algorithms and reaching between the top 1% and 0.1% CADD scores (Kircher *et al.*, 2014). In addition, all variants affect highly conserved amino acid residues and nucleotides, except for a moderately conserved nucleotide in Proband 4. *PAK1* shows fewer missense variants than expected by chance with a z-score of 4.16 (Lek *et al.*, 2016), suggesting that heterozygous missense variants are less tolerated. In addition, *in silico* modelling of protein structures of wild-type and altered *PAK1* revealed that all four identified variants similarly lead to a disturbance of the autoinhibition mechanism (Fig. 1).

Variants Leu470Arg, Ser133Pro and Ser110Thr are located in the interface between the inhibitory switch domain and the catalytic domain (Fig. 1). In each variant, the wild-type residue is replaced by a bulkier amino acid resulting in steric problems ('clashes') with adjacent amino acids, which destabilize the autoinhibitory domain and its interaction with the catalytic domain. Introducing arginine at p.Leu470, proline at p.Ser133, and threonine at p.Ser110 reduces binding by 1.76 kcal/mol, 1.26 kcal/mol, and 0.99 kcal/mol, respectively. The fourth variant, Pro121Ser, is located in the *PAK1* dimer interface formed by the inhibitory switch domains of both subunits (Fig. 1 and Supplementary Fig. 1) and weakens binding by 2.30 kcal/mol. As a reference, an energy change of 1.36 kcal/mol corresponds to a reduction in binding affinity by one order of magnitude indicating that all three variants significantly destabilize the interaction between the inhibitory switch and the catalytic domain. In addition, the Pro121Ser variant is also expected to destabilize the autoinhibitory conformation of the switch domain itself: the rigid Pro121 with its cyclic sidechain is involved in the formation of a kink between two α -helices (Fig. 2K), which is expected to become more flexible in the Ser121

variant. The inhibitory switch domain has been described as the core of the autoregulatory fragment, which appears to inhibit the kinase with one surface and anchor the dimer contact with another. Conformational changes in this highly conserved protein domain are likely to affect protein function. A loss of stability in the autoinhibitory domain, thereby reducing autoinhibition would be supportive of a gain-of-function mode of the observed genetic variants. A *PAK1* variant in the inhibitory switch domain, Leu107Phe, is already known to prevent the interaction between the N-terminal regulatory portion and catalytic domain, leading to kinase activation (Brown *et al.*, 1996).

Discussion

PAK1 is a family member of the serine/threonine p21-activating (PAK) kinases composed of six known members in humans, *PAK1*–6. These proteins are critical effectors that link RhoGTPases to cytoskeleton reorganization and nuclear signalling and other intracellular processes (Manser *et al.*, 1998; Zhao and Manser, 2012; Rane and Minden, 2014). Both *PAK1* and *PAK3* have been reported to control brain size through coordinating neuronal complexity and synaptic properties (Huang *et al.*, 2011). Nonsense and missense variants that are thought to decrease autophosphorylation and activation of *PAK3* have been described in males with X-linked recessive developmental delay (MIM: 300558). Recently, two probands with a neurodevelopmental disorder and *de novo* missense variants in *PAK1* have been described. Their phenotype is similar to the phenotype presented by our probands with developmental delay, macrocephaly, seizures, and ataxic gait (Harms *et al.*, 2018). The described variants p.(Tyr131Cys) and p.(Tyr429Cys) are located in the autoinhibitory and kinase domains of *PAK1* similarly to the *de novo* variants presented in our study. Harms *et al.* (2018) furthermore showed that both variants lead to significantly reduced dimerization, providing evidence for a gain-of-function pathomechanism. Our results on the location of variants and the predicted effects on the protein provide additional evidence for this pathomechanism.

PAK1 is central to a well-described signalling pathway and an involvement in neurodevelopmental disorders was also described for other members of the pathway. Interacting partners of *PAK1*, especially the *PAK1* activators *RAC1* and *CDC42*, have been associated with developmental syndromes (Fig. 3 and Supplementary Table 2). *De novo* pathogenic missense *RAC1* variants are associated with varying degrees of developmental delay, brain malformations, and additional phenotypes in autosomal dominant mental retardation 48 (MIM: 617751). Notably, of the seven reported affected individuals, two were macrocephalic; however, without a clear effect of protein activation. Pathogenic, heterozygous *de novo* or familial variants in *CDC42* cause a highly heterogeneous developmental

Table 1 Clinical features of individuals with predicted missense variants in PAK1

	Proband 1	Proband 2	Proband 3	Proband 4
cDNA change	c.1409T > G	c.397T > C	c.361C > T	c.328T > A
Amino acid change	p.(Leu470Arg)	p.(Ser133Pro)	p.(Pro121Ser)	p.(Ser110Thr)
Ethnicity	Caucasian	Caucasian	Morocco	Sephardi Jew
Age at last exam/Sex	4y/Female	17y/Male	20y/Male	8y/Male
HC last examination	55.5 cm (> P99 + 3.80 SD)	59.8 cm (P98 + 2.07 SD)	61.5 cm (> P99 + 2.95 SD)	59.5 cm (> P99 + 4.93 SD)
BMI	13.9 (P14 – 1.09 SD)	Not measured	24.7 (P84 + 0.98 SD)	15.3 (P33 – 0.45 SD)
Pregnancy	Maternal gestational diabetes, pre-eclampsia	No anomalies	No anomalies	Choroid plexus cyst
Birth at gestational week	30 weeks	32 weeks	34 weeks	40 weeks
Birth parameters	Weight 1120 g (P25 – 0.69 SD) Length 41 cm (P67 + 0.45 SD) HC 27.5 cm (P43 – 0.18 SD)	Weight 2268 g (P86 + 1.07 SD) Length NA HC NA	Weight 2100 g (P34 – 0.4 SD) Length NA HC NA	Weight 2800 g (P3 – 1.87SD) Length NA HC 34.5 cm (P20 – 0.85 SD)
Neonatal period	APGAR 8/9/10 Primary C-section	APGAR NA Spontaneous uncomplicated premature vaginal delivery NICU 4 weeks	APGAR 6/8/9 IRDS, 4 days artificial respiration (CPAP and IPPV)	APGAR NA NA
Congenital anomalies	NICU Partial 2–4 toe syndactyly; long fingers	Partial 2–3 toe syndactyly; macrocephaly	Neonatal jaundice (phototherapy for 3 days)	No anomalies
Postnatal growth (Strauss et al., 2018), HC	At 3 months: HC 37 cm (P89 + 1.2 SD) At 6 months: HC 43.5 cm (P97 + 1.9 SD) At 12 months: HC 48.3 cm (> P97 + 2.75 SD)	At 13 months: HC 52 cm (> P99 + 3.96 SD), length 76 cm (P26 – 0.65SD), weight 10.84 kg (P62 + 0.31SD)	No anomalies At 12 y: HC 59 cm (> P99 + 3.27 SD), length 140 cm (P7 – 1.49 SD)	At 18 months: HC 58 cm (> P99 + 7.76 SD)
Developmental delay	Yes	Yes	Yes	Yes
Intellectual disability	Moderate to severe	Profound	Moderate to severe	Profound
Speech and language	Delayed, no active speech	Non-verbal	Delayed, sentences at age of 10 y	Non-verbal
Mental health disorders	Autistic traits	Autism	ADHD	Autism
Facial dysmorphism/physical signs	Macrocephaly, frontal bossing, thin upper vermillion, broad nasal bridge, low-set posteriorly rotated ears	Craniofacial disproportion	Macrocephaly	Macrocephaly, strabismus
Muscular tone	Hypotonia	Initial hypotonia, later spastic quadriplegia	First year hypotonia	Hypotonia
Walking abilities	Unstable gait	No walking	Walking, mild ataxia	Ataxic, unstable gait
Brain/MRI	MRI: thin corpus callosum, ventriculomegaly, globular and mildly amorphous hippocampi bilaterally	MRI: thin corpus callosum, cerebellar atrophy with widening of the sulci, megalencephaly, ventriculomegaly, mildly small and amorphous hippocampi bilaterally	MRI: thick corpus callosum, non-specific white matter anomalies of the deep white matter, bilateral and parietal, and of splenium of corpus callosum. MRS (spectroscopy): in white matter strongly increased total NAA (not in cortex)	MRI: thick corpus callosum, high bilateral signal intensity in frontal subcortical region
Seizures	At age 19–21 months three febrile seizures, seizures with awareness impairment and myoclonic seizures	Starting age 6 y, atonic, tonic-clonic seizures	One typical febrile seizure (age not known)	Starting age 1.5 y, focal epilepsy
EEG	Irregular basal activity at 6–8 Hz, intermittent beta wave activity, focus in right hemispheric region centroparietal and frontotemporal, spike waves occipital left, focal morphology, without generalization	High-amplitude paroxysmal discharges at the vertex	NA	Sharp waves in frontotemporal regions
Additional features/notes	NA	NA	CSF normal, tremor onset at 10 y, positional tremor and tremor of tongue, no intention tremor, progressive tremor, no pyramidal signs	NA

Percentiles and standard deviations (SD) were calculated using <https://www.pedz.de>. CPAP = continuous positive airway pressure; HC = head circumference; IRDS = intermittent positive pressure ventilation; IRDS = infant respiratory distress syndrome; MRS = magnetic resonance spectroscopy; NA = not available; NAA = N-acetyl aspartate; NICU = neonatal intensive care unit.

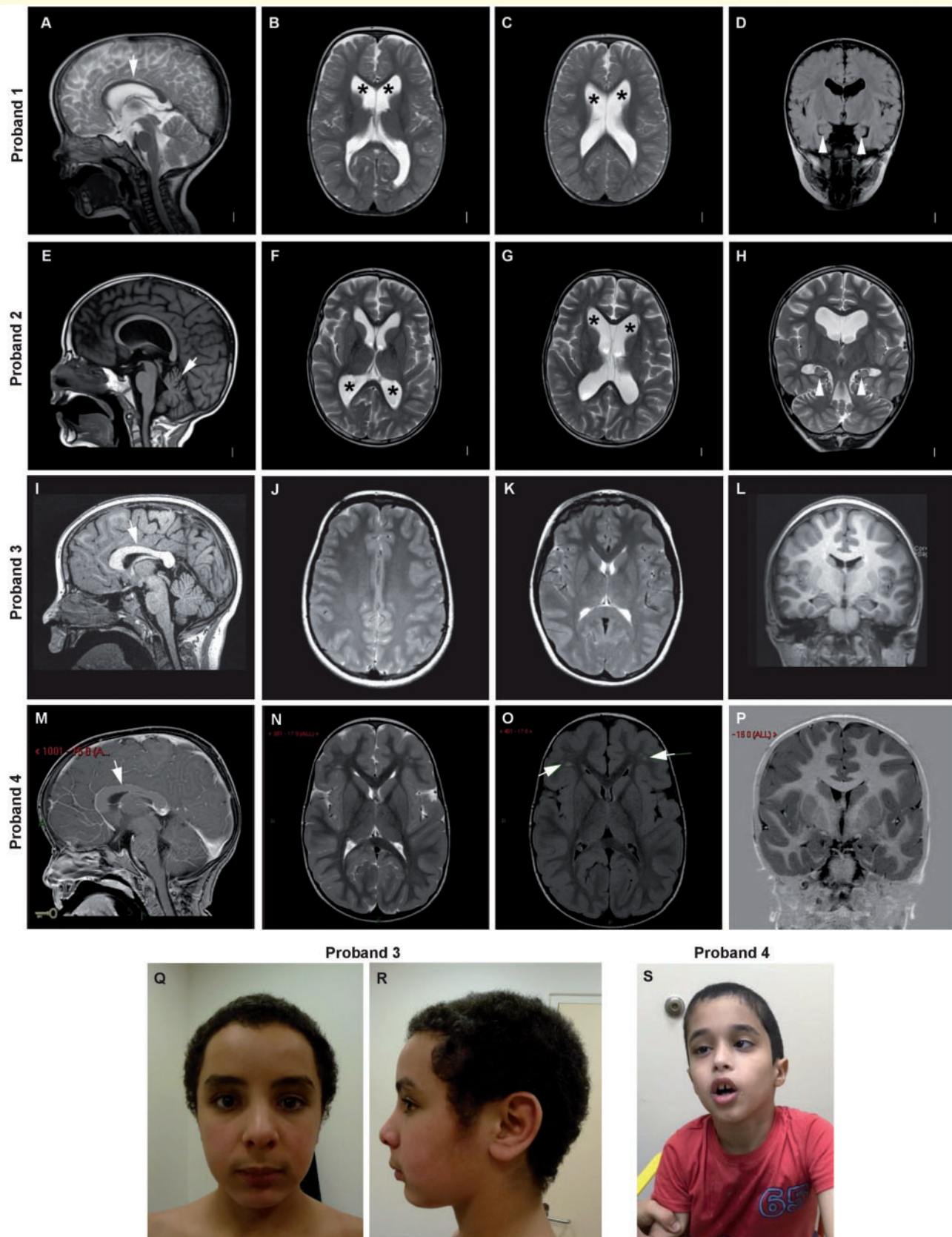


Figure 2 Brain MRI and facial features of individuals with heterozygous *PAK1* mutation. Brain MRIs of Proband 1 at age 2 years (A–D), Proband 2 at age 14 years (E–H), Proband 3 at age 12 years (I–L) and Proband 4 at age 8 years (M–P). Macrocephaly was caused by megalencephaly with or without accompanying ventriculomegaly. (A) T₂ mid-sagittal image showing a thin corpus callosum (arrow). (B and C) T₂ axial images showing ventriculomegaly (asterisks). (D) T₁ coronal image showing globular and mildly amorphous hippocampi bilaterally. (E) T₁

(continued)

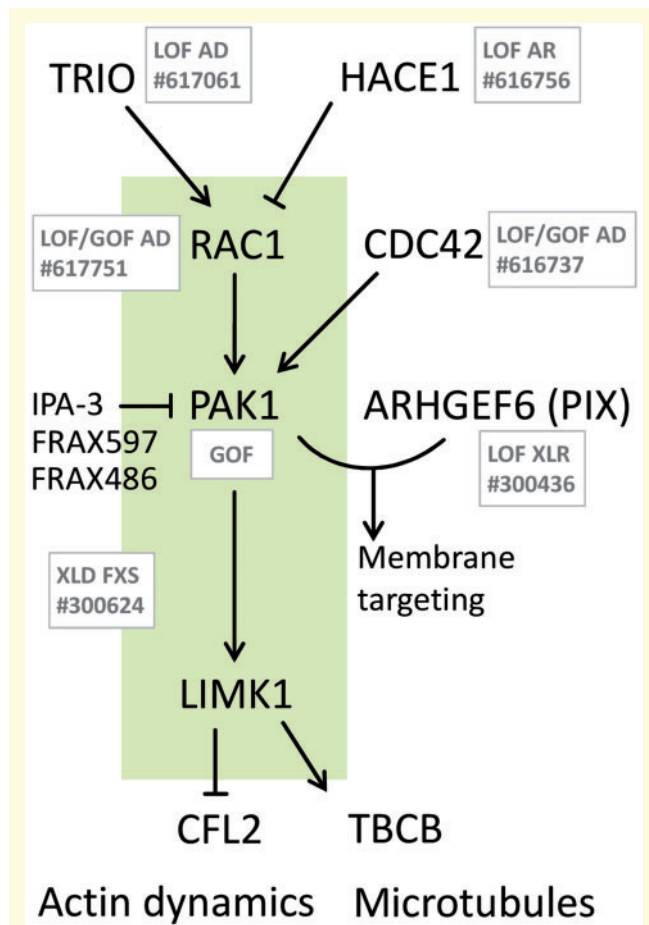


Figure 3 Involvement of the PAK1 pathway in developmental phenotypes. RAC1 and CDC42 are direct activators, TRIO and HACE1 are indirect (via RAC1) regulators of PAK1. ARHGEF6 binds PAK1 for regulation of neurite outgrowth. PAK1 activates LIMK1, the regulator of PAK1 downstream effectors cofilin (CFL2) and tubulin cofactor B. Disorders associated with deactivating and/or activating variants for each gene are indicated in grey with the respective mode of inheritance given (see Supplementary Table 2 for details and phenotypic overlap). Green shaded box indicates activation of RAC1-PAK1-LIMK1 pathway in FXS, where macrocephaly also occurs. Currently available inhibitors of PAK1 are indicated.

disorder (MIM: 616737). Some individuals with *CDC42* variants showed a broad forehead; however again, carrying both activating and deactivating variants.

Variants in *TRIO* and *HACE1*, known interactors of RAC1, are mainly reported as loss-of-function variants (MIM: 617061 and MIM: 616756). Notably, the PAK1-pathway is presumably activated in *HACE1* deficiency neurodevelopmental syndrome (Hollstein *et al.*, 2015) and the disorder resembles many of the symptoms described in this study, excluding macrocephaly, though one *HACE1* patient had a large head circumference at birth (Supplementary Table 2). To determine other interactors of PAK1 we identified genes that show an expression associated with that of PAK1 and that code for proteins that physically interact with PAK1 (Supplementary Fig. 2). Additionally *ARHGEF6* has been associated with a neurodevelopmental disorder (MIM: 300436). *ARHGEF6* encodes the Rac/Cdc42 guanine nucleotide exchange factor 6 (PIX) (Manser *et al.*, 1998), which can bind to PAK1 for the mediation of neurite outgrowth (Rane and Minden, 2014). A role of PAK1 in neuronal growth is also supported by MRI data of our probands. *N*-acetyl aspartate (NAA) is a key metabolite and marker of intact neurons. Increased total levels of NAA were detected in the MRI of Proband 3 and could possibly be related to the increased growth of neurons as a cause of megalencephaly in PAK1-related disorders. Amorphous hippocampi were present in two of four probands (Probands 1 and 2). It has been shown previously that PAK1 is critical in hippocampal synaptic plasticity by the regulation of cofilin activity and the actin cytoskeleton (Asrar *et al.*, 2009). Hence, altered PAK1 activity may result in morphological changes of hippocampi, a feature that could be tested in future patients.

PAK1 is highly expressed in the human cerebellum and cortex and studies have described its role in neuronal migration by activating its downstream targets: LIMK1, cofilins and tubulin cofactor B (Sells *et al.*, 1997; Delorme *et al.*, 2007; Martinelli *et al.*, 2018). PAK1 phosphorylation of tubulin cofactor B is essential for the polymerization of new microtubules, which is important for building and rebuilding neuronal structures (Edwards *et al.*, 1999; Vadlamudi *et al.*, 2005). PAK1 activates LIMK1 that plays a critical role in dendritic spine morphogenesis and brain function by phosphorylation and deactivation of cofilin (Meng *et al.*, 2002). Cofilin can directly bind to actin filaments and promote their disassembly, needed for the reorganization of actin networks during neuronal growth (Chen *et al.*, 2011). Consequently, increased activity of

Figure 2 Continued

mid-sagittal image showing a thin corpus callosum and cerebellar atrophy with widening of the sulci (arrow). (F and G) T₂ axial images showing ventriculomegaly (asterisks). (H) T₂ coronal image showing mildly small and amorphous hippocampi bilaterally. (I) T₁ mid-sagittal image showing a thick corpus callosum (arrow). (J and K) T₂ axial images showing normal lateral ventricles. The white matter signal is slightly hyperintense in the posterior white matter, including the splenium (also present on FLAIR images, not shown). (L) T₁ coronal image showing normal volume and position of the hippocampi. At proton MR spectroscopy, *N*-acetyl aspartate was elevated (not shown). These findings were unchanged 9 months later. (M) T₁ mid-sagittal image showing macrocephaly and a thick corpus callosum (arrow). (N) T₂ axial image showing normal size of the lateral ventricles. (O) FLAIR axial image showing small foci of abnormal signal in frontal white matter may be related to old insult. (P) T₁ coronal image showing normal anatomy of the hippocampi. (Q and R) Photographs of Proband 3 at age 14 years with macrocephaly. (S) Photograph of Proband 4 at age 8 years with macrocephaly, facial muscular hypotonia and strabismus.

PAK1 in our probands would lead to increased activity of LIMK and thereby reduced actin dynamics via cofilin.

Recently, it was shown that the inherited intellectual disability and autism-associated FXS (MIM: 300624) is characterized by activated PAK1 (Pyronneau *et al.*, 2017). Intriguingly, the characteristic loss of the mRNA-binding protein FMR1 increased the abundance and activity of Rac1 in mice. Rac1 activated the kinases Pak1 and Limk1, which inactivated cofilin, thus preventing actin depolymerization dynamics (Hayashi *et al.*, 2007; Pyronneau *et al.*, 2017). Both macrocephaly and seizures are also typically present in FXS, underscoring a similarity of phenotypes in patients with mutations in *PAK1* and FXS.

Another piece of evidence supporting a gain-of-function mechanism for the identified variants in our patients is that *PAK1* homozygous knockout (*Pak1*^{-/-}) mice appear to be viable with no gross abnormalities. Human and mouse *PAK1* genes are extremely well conserved, being 98% identical. *Pak1*^{-/-} mice have some metabolic abnormal phenotypes, mainly increased blood urea levels, increased triglycerides, decreased lean body mass and decreased bone mineral content, and decreased neutrophils; however, no neurodevelopmental abnormalities or abnormal head size were reported (<http://www.mousephenotype.org/data/genes/MGI:1339975>). The fact that loss-of-function variants of *PAK1* are tolerated in human populations (pLI = 0.67) (Karczewski *et al.*, 2016) also indicates that this may not represent a prevailing pathomechanism of *PAK1*-associated disease.

Several inhibitors of PAK1 are currently under development and comprise ATP-competitive inhibitors, such as FRAX597 and FRAX486, which block ATP binding at the catalytic domain of PAK1 (Sampat and Minden, 2018). Dibenzodiazepines inhibit PAK1 by preventing its autophosphorylation (Karpov *et al.*, 2015). If *PAK1*-associated disease proves to exhibit a gain-of-function mechanism, novel options for the treatment of affected patients could arise.

The importance of *PAK1* in neuronal growth and structure, the positions and amino acids affected by the four identified genetic variants and their predicted effects on the protein, the strongly overlapping phenotypes of the affected individuals, as well as previously published data on other members of the *PAK1*-associated pathway allow us to consider that the *de novo* variants in *PAK1* discovered in this study are the cause of a neurodevelopmental disorder characterized by intellectual disability with macrocephaly and seizures.

Web resources

Genematcher, <https://genematcher.org/>
GnomAD, <http://gnomad.broadinstitute.org/>
VARVIS, <https://www.limbus-medtec.com/>
UCSC Genome Browser, <https://genome.ucsc.edu/>

HGMD, https://portal.biobase-international.com/cgi-bin/portal/login.cgi?redirect_url=/hgmd/pro/start.php?
PolyPhen-2, <http://genetics.bwh.harvard.edu/pph2/>
MutationTaster, <http://www.mutationtaster.org/>
CADD, <http://cadd.gs.washington.edu/score>
R2, <https://hgserver1.amc.nl/cgi-bin/r2/main.cgi>
NCBI Pubmed, <https://www.ncbi.nlm.nih.gov/pubmed/>
Pedz, <https://www.pedz.de>
Online Mendelian Inheritance in Man, <http://www.omim.org/>
Genemania, <https://genemania.org>

Acknowledgements

We thank the families and referring physicians for their participation in this study. We thank Julia Hentschel for technical assistance.

Funding

Research reported in this publication was supported by the National Institute of Neurological Disorders and Stroke (NINDS) under award number K08NS092898 and Jordan's Guardian Angels (to G.M.). The content is solely the responsibility of the authors, and does not necessarily represent the official views of the National Institutes of Health. The funding sources had no role in the design and conduct of the study, collection, management, analysis and interpretation of the data, preparation, review or approval of the manuscript, or decision to submit the manuscript for publication.

Competing interests

C.G.-J. is a full-time employee of the Regeneron Genetics Center from Regeneron Pharmaceuticals Inc. and receives stock options as part of compensation. A.C. and C.M. are employed by and receive a salary from ARUP Laboratories. P.B.-T. is a consultant to ARUP Laboratories. The other authors declare no conflict of interest.

Supplementary material

Supplementary material is available at *Brain* online.

References

Asrar S, Meng Y, Zhou Z, Todorovski Z, Huang WW, Jia Z. Regulation of hippocampal long-term potentiation by p21-activated protein kinase 1 (PAK1). *Neuropharmacology* 2009; 56: 73–80.
Boycott KM, Rath A, Chong JX, Hartley T, Alkuraya FS, Baynam G, *et al.* International cooperation to enable the diagnosis of all rare genetic diseases. *Am J Hum Genet* 2017; 100: 695–705.

- Brown JL, Stowers L, Baer M, Trejo J, Coughlin S, Chant J. Human Ste20 homologue hPAK1 links GTPases to the JNK MAP kinase pathway. *Curr Biol* 1996; 6: 598–605.
- Chen S-Y, Huang P-H, Cheng H-J. Disrupted-in-schizophrenia 1-mediated axon guidance involves TRIO-RAC-PAK small GTPase pathway signaling. *Proc Natl Acad Sci* 2011; 108: 5861–6.
- De Ligr J, Willemsen MH, van Bon BWM, Kleefstra T, Yntema HG, Kroes T, et al. Diagnostic exome sequencing in persons with severe intellectual disability. *N Engl J Med* 2012; 367: 1921–9.
- Delorme V, Machacek M, DerMardirossian C, Anderson KL, Wittmann T, Hanein D, et al. Cofilin activity downstream of Pak1 regulates cell protrusion efficiency by organizing lamellipodium and lamella actin networks. *Dev Cell* 2007; 13: 646–62.
- Edwards DC, Sanders LC, Bokoch GM, Gill GN. Activation of LIM-kinase by Pak1 couples Rac/Cdc42 GTPase signalling to actin cytoskeletal dynamics. *Nat Cell Biol* 1999; 1: 253.
- Harms FL, Kloth K, Bley A, Denecke J, Santer R, Lessel D, et al. Activating mutations in PAK1, encoding p21-activated kinase 1, cause a neurodevelopmental disorder. *Am J Hum Genet* 2018; 103: 579–91.
- Hayashi ML, Rao BS, Seo J-S, Choi H-S, Dolan BM, Choi S-Y, et al. Inhibition of p21-activated kinase rescues symptoms of fragile X syndrome in mice. *Proc Natl Acad Sci* 2007; 104: 11489–94.
- Hollstein R, Parry DA, Nalbach L, Logan CV, Strom TM, Hartill VL, et al. HACE1 deficiency causes an autosomal recessive neurodevelopmental syndrome. *J Med Genet* 2015; 52: 797–803.
- Huang W, Zhou Z, Asrar S, Henkelman M, Xie W, Jia Z. p21-Activated kinases 1 and 3 control brain size through coordinating neuronal complexity and synaptic properties. *Mol Cell Biol* 2011; 31: 388–403.
- Karczewski KJ, Weisburd B, Thomas B, Solomonson M, Ruderfer DM, Kavanagh D, et al. The ExAC browser. Displaying reference data information from over 60 000 exomes. *Nucl Acids Res* 2016; 45: D840–5.
- Karpov AS, Amiri P, Bellamacina C, Bellance M-H, Breitenstein W, Daniel D, et al. Optimization of a dibenzodiazepine hit to a potent and selective allosteric PAK1 inhibitor. *ACS Med Chem Lett* 2015; 6: 776–81.
- Kircher M, Witten DM, Jain P, O’roak BJ, Cooper GM, Shendure J. A general framework for estimating the relative pathogenicity of human genetic variants. *Nat Genet* 2014; 46: 310.
- Lei M, Lu W, Meng W, Parrini M-C, Eck MJ, Mayer BJ, et al. Structure of PAK1 in an autoinhibited conformation reveals a multi-stage activation switch. *Cell* 2000; 102: 387–97.
- Lek M, Karczewski KJ, Minikel EV, Samocha KE, Banks E, Fennell T, et al. Analysis of protein-coding genetic variation in 60,706 humans. *Nature* 2016; 536: 285.
- Manser E, Loo T-H, Koh C-G, Zhao Z-S, Chen X-Q, Tan L, et al. PAK kinases are directly coupled to the PIX family of nucleotide exchange factors. *Mol Cell* 1998; 1: 183–92.
- Martinelli S, Krumbach OHF, Pantaleoni F, Coppola S, Amin E, Pannone L, et al. Functional dysregulation of CDC42 causes diverse developmental phenotypes. *Am J Hum Genet* 2018; 102: 309–20.
- Maulik PK, Mascarenhas MN, Mathers CD, Dua T, Saxena S. Prevalence of intellectual disability. A meta-analysis of population-based studies. *Res Dev Disabil* 2011; 32: 419–36.
- Meng Y, Zhang Y, Tregoubov V, Janus C, Cruz L, Jackson M, et al. Abnormal spine morphology and enhanced LTP in LIMK-1 knockout mice. *Neuron* 2002; 35: 121–33.
- Parrini MC, Lei M, Harrison SC, Mayer BJ. Pak1 kinase homodimers are autoinhibited in trans and dissociated upon activation by Cdc42 and Rac1. *Mol Cell* 2002; 9: 73–83.
- Pettersen EF, Goddard TD, Huang CC, Couch GS, Greenblatt DM, Meng EC, et al. UCSF Chimera—a visualization system for exploratory research and analysis. *J Comput Chem* 2004; 25: 1605–12.
- Pirruccello M, Sondermann H, Pelton JG, Pellicena P, Hoelz A, Chernoff J, et al. A dimeric kinase assembly underlying autophosphorylation in the p21 activated kinases. *J Mol Biol* 2006; 361: 312–26.
- Pyronneau A, He Q, Hwang J-Y, Porch M, Contractor A, Zukin RS. Aberrant Rac1-cofilin signaling mediates defects in dendritic spines, synaptic function, and sensory perception in fragile X syndrome. *Sci Signal* 2017; 10: eaan0852.
- Rane CK, Minden A. P21 activated kinases. Structure, regulation, and functions. *Small GTPases* 2014; 5: e28003.
- Sampat N, Minden A. Inhibitors of the p21 activated kinases. *Curr Pharmacol Rep* 2018; 4: 238–49.
- Sells MA, Knaus UG, Bagrodia S, Ambrose DM, Bokoch GM, Chernoff J. Human p21-activated kinase (Pak1) regulates actin organization in mammalian cells. *Curr Biol* 1997; 7: 202–10.
- Trujillano D, Bertoli-Avella AM, Kandaswamy KK, Weiss MER, Köster J, Marais A, et al. Clinical exome sequencing. Results from 2819 samples reflecting 1000 families. *Eur J Hum Genet* 2017; 25: 176.
- Vadlamudi RK, Barnes CJ, Rayala S, Li F, Balasenthil S, Marcus S, et al. p21-activated kinase 1 regulates microtubule dynamics by phosphorylating tubulin cofactor B. *Mol Cell Biol* 2005; 25: 3726–36.
- Vissers LE, Gilissen C, Veltman JA. Genetic studies in intellectual disability and related disorders. *Nature Rev Genet* 2016; 17: 9.
- Xiong P, Zhang C, Zheng W, Zhang Y. BindProfX. Assessing mutation-induced binding affinity change by protein interface profiles with pseudo-counts. *J Mol Biol* 2017; 429: 426–34.
- Zhao Z-S, Manser E. PAK family kinases. Physiological roles and regulation. *Cell Logist* 2012; 2: 59–68.